



Published in final edited form as:

Nat Commun. ; 5: 4858. doi:10.1038/ncomms5858.

A sequence variant in human *KALRN* impairs protein function and coincides with reduced cortical thickness

Theron A. Russell¹, Katherine D. Blizinsky^{1,2}, Derin J. Cobia², Michael Cahill¹, Zhong Xie¹, Robert A. Sweet^{3,4}, Jubao Duan^{5,6}, Pablo V. Gejman^{5,6}, Lei Wang^{2,7}, John G. Csernansky², and Peter Penzes^{1,2}

¹Department of Physiology, Northwestern University Feinberg School of Medicine, Chicago, Illinois 60611, USA

²Department of Psychiatry and Behavioral Sciences, Northwestern University Feinberg School of Medicine, Chicago, Illinois 60611, USA

³Department of Psychiatry, University of Pittsburgh School of Medicine, Pittsburgh, Pennsylvania 15213, USA

⁴Department of Neurology, University of Pittsburgh School of Medicine, Pittsburgh, Pennsylvania 15213, USA

⁵Department of Psychiatry and Behavioral Sciences, University of Chicago, Chicago, Illinois 60637, USA

⁶Department of Psychiatry and Behavioral Sciences, North Shore University HealthSystem, Evanston, Illinois 60208, USA

⁷Department of Radiology, Northwestern University Feinberg School of Medicine, Chicago, Illinois 60611, USA

Abstract

Dendritic spine pathology is a key feature of several neuropsychiatric disorders. The Rac1 guanine nucleotide exchange factor kalirin-7 is critical for spine morphogenesis on cortical pyramidal neurons. Here we identify a rare coding variant in the *KALRN* gene region that encodes the catalytic domain, in a schizophrenia patient and his sibling with major depressive disorder. The D1338N substitution significantly diminished the protein's ability catalyze the activation of Rac1. Contrary to wild-type kalirin-7, kalirin-7-D1338N failed to increase spine size and density. Both subjects carrying the polymorphism displayed reduced cortical volume in the superior temporal sulcus (STS), a region implicated in schizophrenia. Consistent with this, mice with reduced kalirin expression showed reduced neuropil volume in the rodent homolog of the STS. These data suggest

Users may view, print, copy, and download text and data-mine the content in such documents, for the purposes of academic research, subject always to the full Conditions of use:http://www.nature.com/authors/editorial_policies/license.html#terms

Correspondence and requests for materials should be addressed to P.P. (p-penzes@northwestern.edu).

Author contributions: P.P., J.G.C., and P.V.G. conceived the study; T.A.R., K.D.B., D.J.C., M.C., and Z.X. designed experiments and collected and analyzed data; J.D. and P.V.G. coordinated human genetic studies; L.W., D.J.C., and J.G.C. coordinated MRI studies; R.A.S. gave conceptual advice; T.A.R., K.D.B., and P.P. wrote the manuscript.

Competing financial interests: The authors declare no competing financial interests.

that single amino acid changes in proteins involved in dendritic spine function can have significant effects on the structure and function of the cerebral cortex.

Keywords

synapse; neuropil; schizophrenia; MRI; gene; dendritic spine

Introduction

In the mammalian forebrain, most excitatory synapses are located on dendritic spines, small protrusions of dendrites¹. Spine morphology modulates synaptic properties and the ability to undergo plasticity^{2, 3}. Spine plasticity driven by changes in synaptic activity contributes to the remodeling of neural circuits during postnatal development, including experience-dependent plasticity which occurs throughout life. Spine enlargement parallels various forms of potentiation, including long-term potentiation (LTP), whereas long-term depression (LTD) seems associated with spine shrinkage⁴. Accordingly, spines can undergo morphological changes in live animals following changes in sensory input, and during social interactions, stress, environmental enrichment, learning and other behavioral conditions⁵.

Abnormal synaptic connectivity is a well-established characteristic of several psychiatric disorders, including schizophrenia, but the exact molecular mechanisms underlying synaptic pathogenesis are not known^{6, 7}. Mounting evidence indicating that known schizophrenia susceptibility genes regulate spines strongly reinforces the hypothesis that perturbations in the molecular pathways underlying spine plasticity are deeply involved in the development and progression of schizophrenia⁷. Because dendrites and spines make up a significant fraction of the cortical neuropil, it has been hypothesized that changes in dendrite and spine number and morphology may lead to alterations in cortical thickness measures, a finding reported in several mental disorders, including schizophrenia⁸.

Changes in the actin cytoskeleton are heavily implicated in the morphological alteration of spines and are controlled by proteins of the small GTPase family⁹. These proteins serve as molecular switches that fluctuate between GTP-bound active and GDP-bound inactive states, and are controlled by guanine nucleotide exchange factors (GEFs) and GTPase activating proteins (GAPs)¹⁰. One of these small GTPase regulators, the Rac-GEF commonly known as kalirin-7 but sometimes referred to as Duo, has been identified as both playing a critical role in spine morphogenesis and associated with increased psychiatric risk^{7, 11}. Kalirin-7, encoded by the human *KALRN* gene and the rodent *Kalrn* gene, is the most highly expressed kalirin protein isoform in the adult rodent brain, with its highest expression levels in the cerebral cortex and hippocampus^{12, 13}. It is primarily localized to spines, and its expression levels rise during a period corresponding to that of synaptogenesis^{12, 14}. Kalirin-7 catalyzes the activation of Rac1, thereby allowing it to bind to p21-activated kinase (PAK), which in turn facilitates actin remodeling^{15, 16}. Overexpression of kalirin-7 results in increased spine number¹⁵, and neurons in which kalirin-7 has been knocked down display reductions in spine density¹⁷. Kalirin-7 is also required for NMDA receptor-dependent structural plasticity and concomitant increases in

synaptic AMPA receptor expression^{17, 18} and interacts with the products of schizophrenia susceptibility genes *DISC1*¹⁹, *NRG1*, and *ERBB4*²⁰ to regulate spine and dendrite plasticity. *Kalrn* knockout mice display a periadolescent reduction in cortical dendritic spine number and reduced dendritic complexity, as well as deficits in working memory that emerge in adolescence^{18, 21}. *KALRN* has been associated with schizophrenia risk through re-sequencing and association analysis²² and post-mortem analyses of patients' cortical *KALRN* mRNA and protein levels^{23, 24}.

Recent large scale studies revealed that rare sequence variants, such as copy number variations and exonic mutations in glutamatergic synaptic plasticity genes are enriched in subjects with schizophrenia^{25, 26}. However, functional analyses of such sequence variants, especially exonic mutations, present in human subjects in synaptic plasticity genes have not been extensively performed. In addition, the relationship between such molecular and cellular variations and macroscopic brain morphometric phenotypes has not been examined. As an initial step in this direction, we sought to identify coding and potentially functionally important variants in *KALRN* in human subjects, assess the functional impact of such variations, and explore neuromorphometric parameters in carrier subjects. We thus sequenced specifically in the region that codes for the kalirin protein's Rac1-GEF catalytic domain. We identified one such variant which significantly impaired protein function and neuronal morphology. Interestingly, the subjects carrying this variant displayed reduced cortical thickness in the caudal portion of the superior temporal sulcus. Consistent with this, mice lacking the *kalrn* gene show reduced cortical thickness, suggesting a potential link between molecular and cellular alterations and macroscopic neuromorphological phenotypes.

Results

Identification of *KALRN* sequence variants

We screened for missense sequence variants in exons 23-28 of human *KALRN* (Figure 1a), which encode the Dbl homology (DH) portion of its gene products' Rac1-GEF enzymatic domain, in a cohort of well-characterized schizophrenia subjects. Sequencing and automated indel/SNP analysis of these exons led to the identification of a rare coding variant, NC_000003.12:g.124462620G>A (NP_001019831.2:p.D1338N), located in the Rac1-GEF domain of *KALRN* in a single subject with schizophrenia (KAL-SCZ) (Figure 1b; Supplementary Table 1). This initial screen was followed by a second screen for the variant in siblings and non-diseased controls (Supplementary Table 2). The only carrier for the variant identified in this screen was a sibling of KAL-SCZ (KAL-SIB), who while not schizophrenic, had been diagnosed with major depressive disorder and alcohol and cocaine dependence. This known minor allele (rs139954729) is predicted by PolyPhen²⁷ to be probably damaging, with a score of 0.981 (sensitivity: 0.75; specificity: 0.96). It was not found in European ancestry subjects in a large exome sequencing data set, NHLBI GO Exome Sequencing Project (ESP) (n=4300; <http://evs.gs.washington.edu/EVS/>). It is also found in African American subjects (n=4404 chromosomes), but with a very low population frequency (0.044%). We could not establish the statistical evidence for the association with schizophrenia due to the limited sample size and incidence of the variant. Nevertheless, we

sought to determine whether it would lead to cellular phenotypes, given that the variant was identified in a schizophrenia patient and his sibling with other neuropsychiatric disorders, as well as its low population frequency and the predicted deleterious property.

Biochemical characterization of the D1338N variant

The p.D1338 residue is located in the Rac1-GEF domain of KALRN, and is highly conserved across species in related protein family members, so we hypothesized that a substitution that changes the charge from an acidic to a slightly basic residue in this domain is likely to affect protein function. To determine whether this would be the case, we transfected hEK-293 cells with a cDNA homologous to either the human major allele (referred to hereafter as “wildtype kalirin-7”) or D1338N kalirin-7 constructs and performed a Rac1 activation affinity assay (Figure 2a; Supplementary Fig. 1). As expected, overexpression of wildtype kalirin-7 induced approximately a fourfold increase in Rac1-GTP levels compared to untransfected cells (Figure 2b). While overexpression of the D1338N variant led to an increase in Rac1 activation as compared to the untransfected condition, the degree of activation was significantly less than that induced by wildtype kalirin-7. These results indicate that the D1338N kalirin-7 variant is impaired with respect to the protein's ability to catalyze the exchange of GDP for GTP bound to Rac1.

As many of the downstream effectors of Rac1 are known to cause remodeling of the actin cytoskeleton, we reasoned that a kalirin-7 variant that has impaired GEF activity would also be less able to stimulate actin polymerization. We have previously shown that membrane ruffling, a morphological indicator of actin polymerization, can be induced by expression of either full length kalirin-7 protein or the kalirin-7 GEF domain alone¹⁴. Therefore, we examined the effect of the D1338N variant on membrane ruffling in COS-7 cells (Figure 2c). The majority of cells expressing wildtype kalirin-7 exhibited membrane ruffling along greater than 80% of their perimeters, representing a significantly greater degree of actin polymerization than that induced by kalirin-7-D1338N (Figure 2d). Thus, the kalirin-7-D1338N variant's diminished capacity for Rac1 activation has functional consequences in the context of cytoskeletal reorganization.

Neuronal morphology in kalirin-7-D1338N expressing neurons

The processes of dendritic spine maturation, excitatory synapse potentiation, and de novo spine formation are all dependent on remodeling of the actin cytoskeleton^{3, 28}. The requirement of kalirin-7 in regulating these processes in forebrain pyramidal neurons has been well established^{11, 13}. As such, we sought to determine whether the D1338N substitution would impair kalirin-7's ability to promote spine growth and development (Figure 3a). In mature cortical pyramidal neurons (21-28 DIV), overexpression of kalirin-7-D1338N failed to enhance spine density and area, whereas wildtype kalirin-7 overexpression increased both spine parameters (Figure 3b). These data indicate that the D1338N variant not only impacts kalirin-7 protein function, but also has severe effects on spine structural plasticity.

MR imaging of D1338N carriers

Spine morphology is thought to contribute to brain neuropil volume, and post-mortem analyses and structural MR imaging studies of the brains of patients have provided evidence for reduced spine density and cortical thickness in the prefrontal and auditory association cortices in schizophrenia. To explore whether the subjects carrying the kalirin-7-D1338N variant displayed unique neuromorphometric features, we compared MRI measures of cortical thickness between the carrier subjects and non-carriers. This preliminary comparison suggested that both the subject with schizophrenia (KAL-SCZ) and the sibling with depression (KAL-SIB) had reduced cortical thickness in the posterior banks of the left superior temporal sulcus (STS) as compared with the means of comparison groups of schizophrenia subjects (SCZ), their unaffected siblings (SCZ-SIB), and control subjects (CON) (Figure 4a, b).

Thinner cortex in *Kalrn*-deficient mice

Because a causal relationship cannot be established in this case, we sought to determine whether reduced kalirin signaling in animal models could result in cortical morphological phenotypes consistent with the neuroimaging human phenotypes. We have previously reported that total knockout of the *Kalrn* gene in mice leads to reduced cortical thickness, as measured in the frontal cortex^{18, 21}. We therefore analyzed cortical neuropil area in the secondary auditory and temporal association cortices of *Kalrn* heterozygote mice, which better mimic the reduced kalirin signaling of the kalirin-7-D1338N variant (Figure 4c). We labelled cell bodies by performing Nissl staining on coronal sections from 12-week-old mice, and defined neuropil as the area of the tissue that was devoid of stain. *Kalrn* heterozygotes exhibited a significant reduction in neuropil area as compared to wildtypes (Figure 4d) ($92.4 \pm 0.8\%$ of wildtype area). These data indicate the necessity of intact functional kalirin expression for normal cortical morphology.

Discussion

Recent genomic studies have revealed extensive interindividual variability and diversity in the human genome, including common and rare variants, missense and nonsense mutations, and copy number variants^{29, 30}. Genome-wide association and copy number variation studies of schizophrenia and other psychiatric disorders have identified many new disease susceptibility genes involving both common single nucleotide polymorphisms (SNPs) and rare disease variants, most of which contribute small effects³¹. In addition, variations in a number of genes have been associated with mental disorders such as schizophrenia^{32, 33}. It has been suggested that variations that increase risk for mental disorders cluster in gene networks that controls the synapse development and plasticity³⁴. However, few studies have examined sequence variation in human genes encoding synaptic proteins, their molecular and cellular functional consequences, and their potential impact on human brain neuroimaging and phenotypes.

In the current study, we have established the presence of a rare KALRN sequence variant in a patient-sibling pair, which results in a single amino acid change in the kalirin-7 protein's catalytic GEF domain. Although we did not establish this variant as a risk for schizophrenia,

it is predicted to be deleterious and present at a very low frequency in the human population. Additionally, while the sibling carrying the variant did not present with schizophrenia, she had been diagnosed with major depressive disorder, the treatment of which has been linked to increased dendritic spine formation³⁵. Pleiotropy is commonly seen in psychiatric disorders and other complex traits (reviewed in Duan et al.³¹). A schizophrenia susceptibility locus may be associated with not only other psychiatric disorders^{36, 37}, but also some other non-psychiatric disorders, such as multiple sclerosis³⁸ and cardiovascular-disease³⁹. Among psychiatric disorders, such shared genetic susceptibility may be due the shared subphenotypes. Symptoms of mood disorder are common among individuals with schizophrenia⁴⁰, and they are also observed in their relatives at rates higher than those observed in the general population. Additionally, in young adults, depression may be a prodromal sign of psychosis⁴¹. Moreover, variations in clusters of genes, including *KALRN*, implicated in schizophrenia and psychotic bipolar disorder etiology may impact resting state functional activity in affected individuals and first-degree relatives. This attests to the impact of common and rare genetic variation on measurable functional outcomes potentially related to disease phenotypes⁴². One hypothesis for the minor allelic variant in *KALRN* would be that this variant alters cortical thickness, a subphenotype that manifests as schizophrenia or major depressive disorder depending on other genetic modifiers or different individual genetic backgrounds.

At the cellular level the slightly altered protein affects phenotypes, particularly with regard to dendritic spines, in a manner similar to that of kalirin-7 proteins that lack a functional GEF domain¹⁵, as well as those which are incapable of being phosphorylated by upstream signaling proteins¹⁷. Therefore, it stands to reason that altered function in proteins in the kalirin-7 signaling pathway could also cause dendritic spine dysfunction, and, at the anatomical level, cortical thinning. It has previously been shown that kalirin-7 interacts with DISC1¹⁹, and that it is a necessary component of pathways downstream of both NRG1/ERBB4 and 5-HT2A serotonin receptors^{43, 44}. DISC1 variants associated with schizophrenia correlate with reduced cortical thickness in several regions independent of psychiatric diagnosis^{45, 46}. Knockdown of DISC1 in cultured cortical neurons also results in diminished dendritic spine number¹⁹, and frontal cortex pyramidal neurons in mice carrying DISC1 missense variants or truncations display reduced spine number and dendrite length than those in wildtypes^{47, 48}. Similarly, patients carrying a schizophrenia-associated minor NRG1 allele have reduced superior temporal gyrus volumes as compared to patients carrying the major allele⁴⁹, and mice lacking CNS expression of *ErbB2* and *ErbB4* exhibit reduced dendritic spine density in frontal cortex pyramidal neurons⁵⁰. Furthermore, kalirin-7 has been shown to be essential for 5-HT2A receptor-induced dendritic spine growth⁴⁴. Antagonism of the 5-HT2A receptor is considered to be an important mechanism of the action of atypical antipsychotic drugs⁵¹, and schizophrenic patients consistently exhibit decreased levels of these receptors in several cortical regions⁵².

We have previously demonstrated that *Kalrn* null mice have decreased spine number and dendritic arborization as compared to wild-types^{18, 21}, and we show here that they have thinner temporal association cortices. Interestingly, the human subjects carrying this variant have a thinner cortex in the STS. The STS is part of a network that includes the medial

prefrontal cortex and amygdala and is involved in aspects of social cognition, including empathy and theory of mind. Patients show abnormal activation of this network during tasks involving the rating of emotional valence in facial expression⁵³, and flat affect item score is negatively correlated with performance on these tasks⁵⁴. While the scope of our analyses is limited by statistical power and does not demonstrate a causal relationship between p.D1338N and specific endophenotypes in carriers, our published and current data on *Kalrn* knockout mice may fill in the gap to some extent. Mouse knockout data suggest a causal relationship between reduced kalirin function and the regulation of both neuropil size and cortical morphology^{18, 21}. Since such morphological alterations are reminiscent of the structural abnormalities seen in schizophrenic patients^{55, 56}, the role of kalirin in regulating cortical thickness in humans and animal models should be explored further.

During normal development, cortical pyramidal neurons undergo a period of synaptic pruning during adolescence to refine connections before reaching a steady state level in adulthood⁵⁷. This pruning is exaggerated in schizophrenia, and diminished synaptic density, along with less extensive dendritic arborization and smaller pyramidal neuron soma size, is thought to be one of the cellular morphological changes responsible for the decreased cortical gray matter observed in patients^{58, 59, 60}. Post-mortem analyses of brains from schizophrenia patients also demonstrate a reduction in the density of pyramidal neuron dendritic spines in several regions of the cortex, including the dorsolateral prefrontal cortex, the anterior cingulate cortex, and the superior temporal gyrus^{23, 61}.

There are important caveats in this study. It should be noted that neither causality nor an association between the p.D1338N variant and any particular phenotype are established in this particular case, due to only two identified carriers. A more definitive test of association would require a large population case-control sample. Nevertheless, our study is one of the first to demonstrate that rare putatively deleterious variants in *KALRN* can lead to phenotypic changes relevant to schizophrenia. Our results are significant in the context of known supporting evidence for the association of both common and rare variants in *KALRN* with schizophrenia. The most significant association of a common variant in *KALRN* in the Psychiatric Genomics Consortium schizophrenia GWAS data set had a p-value of 5×10^{-462} . Although the associations of common *KALRN* variants with schizophrenia have not reached genome-wide significance, they have been observed in other previous GWAS using different ethnic samples^{63, 64}. Resequencing *KALRN* in a Japanese sample further suggested that rare (MAF<1%) putatively functional missense SNPs may also contribute to schizophrenia risk²². Finally, the preliminary, uncorrected STS finding should be treated with caution. The effect of *KALRN* on cortical thickness may be relatively weak therefore requiring more subjects for increased statistical power.

It should be noted that there have been no single rare coding SNPs that are identified to show a statistically significant association with schizophrenia, even in large exome sequencing projects^{25, 26}. This does not exclude the possibility that some rare functional variants in certain genes do contribute to susceptibility, and intriguingly, rare coding variants are found to be enriched in synaptic genes^{25, 26}. Our study focuses on the functionality of the *KALRN* gene and one of its variants, rather than association evidence. We have shown that relationships could in principle be drawn between rare genetic sequence

variants and neuroimaging and diagnostic phenotypes, given the appropriate number of subjects. Knowledge about the cellular and circuit-level impact of rare genetic variants in human subjects may in future point to disease mechanisms: specific molecular domains or functions, such as enzymatic domains, protein-protein interaction motifs, or phosphorylation sites, affected by amino acid changes could provide clues to the downstream/upstream members of the pathway.

When done at a suitable scale, this approach may provide insight into the pathogenesis of mental disorders. The approach we have taken could be a blueprint for larger scale studies that combine human genetics, cellular and molecular analysis of impact of mutations, and analysis of cognitive, behavioral, and neuromorphometric measures in carriers.

Methods

Human subjects

Study participants were recruited through the Conte Center for the Neuroscience of Mental Disorders (CCNMD) at Washington University in St. Louis. Participants included individuals with schizophrenia based on Diagnostic and Statistical Manual of Mental Disorders, Ed IV (DSM-IV-TR) criteria ($n = 127$), and their non-affected siblings and healthy control participants ($n = 246$). A subset of these participants also elected to undergo structural MR imaging; their demographic information is as follows: patients (SCZ), $n = 33$, 9 females and 24 males, mean age of 24.3 ± 4.0 years; siblings (SCZ-SIB), $n = 40$, 20 females and 20 males; mean age of 23.6 ± 3.7 years; and controls (CON), $n = 25$, 11 females and 14 males, mean age of 20.3 ± 4.9 years. Details of the recruiting process are discussed elsewhere^{65, 66}. All patients provided signed consent, and all activities and procedures were approved by the Washington University in St. Louis Institutional Review Board.

Genomic DNA sequencing

PCR amplification of *KALRN* exons 23-28 and adjacent intronic regions from genomic DNA samples from 127 individuals with schizophrenia and 246 siblings and controls, followed by resequencing and automated indel/SNP analysis, was performed by Beckman Coulter Genomics (Danvers, Massachusetts) on an ABI3730 capillary sequencer. PCR primer sequences are listed in Supplementary Table 3.

Primary neuronal cultures

High density cortical neuron cultures were prepared from Sprague-Dawley rat E18 embryos as described previously⁶⁷. Pooled cortices were minced and cells were dissociated in a papain solution containing DNaseI, L-cysteine, and EDTA (all from Sigma-Aldrich, St. Louis, Missouri). Cells were further dissociated mechanically and then strained, followed by counting of viable cells. Neurons were plated at a density of 3×10^5 cells per well onto coverslips coated with poly-D-lysine (0.2 mg/ml, Sigma-Aldrich) in a 12-well plates, in plating media (feeding media plus 5% fetal calf serum). After 1 hour, the media was changed to feeding media (Neurobasal media supplemented with B27 (Life Technologies, Grand Island, New York) and 0.5 mM glutamine). 200 μ M D, L-amino-phosphonovalerate (Abcam, Cambridge, Massachusetts) was added to the media 4 days later.

Plasmid Transfections

The plasmid encoding myc-kalirin-7, generated by subcloning of rat kalirin-7 cDNA pSCEP. Myc and then into pEAK10. His, was described previously¹⁴. The D1338N kalirin-7 variant was created by site-directed mutagenesis using the QuickChange II XL mutagenesis kit (Agilent Technologies, Santa Clara, California). The sequence of the forward mutagenesis primer was 5'-GGCAACATCCAAGAGATCTACAATTTCCATAACAACATC-3'. Cortical neurons (DIV 24-26) were transfected with 4-6 μ g of the appropriate cDNAs for 4 hours in Neurobasal medium in the presence of Lipofectamine 2000 according to the manufacturer's protocol.

COS-7 and hEK293 cells were grown to ~40% confluency in Dulbecco's modified Eagle's medium (DMEM) with 10% fetal bovine serum and penicillin/streptomycin. Cells were then transfected with appropriate cDNAs in DMEM media without antibiotics or serum using Lipofectamine 2000. Cells were transfected when they reached ~40% confluency and were ~95% confluent at the time of harvesting.

Rac1 activation assay

Transfected hEK293 cells were harvested when they reached ~95% confluency. Active Rac1 levels were assessed using a Rac1 Activation Assay Kit (Millipore, Billerica, Massachusetts) following the manufacturers' protocol with normalization to total Rac1 as described previously¹⁷. Antibodies against c-myc (1:500, Santa Cruz Biotechnology, Dallas, Texas) and β -actin (1:4000, Sigma-Aldrich) were used to control for levels of exogenously expressed protein. Blots were then analyzed with ImageJ⁶⁸.

Membrane ruffling analysis

Analysis of membrane ruffling, a process induced by actin polymerization, was performed in COS-7 cells expressing either wildtype or mutant myc-tagged kalirin-7. Following fixation, cells were immunostained with an anti-myc antibody (Santa Cruz), and F-actin was visualized by incubation with Oregon Green 488-conjugated phalloidin (Life Technologies). Cells expressing myc-tagged protein were imaged using a confocal microscope (Zeiss LSM5 Pascal), and images were analyzed using ImageJ. A membrane ruffle was defined as an actin-rich undulating membrane protrusion folding back from the adherent surface of a cell.

Analysis of sequence variants in neurons

Quantitative analysis of spine number and morphology (area, breadth and length) in cortical pyramidal neurons overexpressing the wildtype *KALRN* or its associated mutants was performed using an approach we have described previously^{16, 17, 21, 44}. Cortical neurons cultured on coverslips of postnatal age DIV 24-26 (corresponding to adolescence) were transfected with pEGFP-N2 (Clontech, Mountain View, California) to express green fluorescent protein (GFP) to visualize cell morphology, either alone or together with myc-tagged kalirin-7 for 48 hrs. Neurons were then fixed and immunostained to visualize spine morphology. Briefly, neurons were fixed with 4% formaldehyde in 4% sucrose/phosphate

buffered saline (PBS), followed by ice cold methanol. After permeabilization and blocking in a solution of 2% normal goat serum/0.1% Triton X-100/PBS, neurons were incubated with an antibody against GFP (1:1000, Millipore), and an anti-myc antibody (1:1000, Santa Cruz) to visualize myc-tagged kalirin-7. Neurons were then washed, incubated with Alexa-Fluor 488- and Alexa-Fluor 568-conjugated secondary antibodies, and mounted onto slides with ProLong Gold Antifade mounting medium. Neurons transfected with the mutation construct were compared to neurons expressing the wild type gene or GFP only. Expression levels of exogenous protein were normalized to GFP, and only cells that express equal levels of exogenous protein, with consistent subcellular targeting, were analyzed. Healthy neurons expressing both GFP and myc-tagged protein were imaged using a 63× oil immersion objective on a confocal microscope (Zeiss LSM5 Pascal). Z stacks of three to eight images, averaged 4 times, were taken at 0.37 μm intervals, with a 1024 × 1024 pixel resolution at a scan speed of 3 s per section. Cultures that were directly compared were stained and imaged simultaneously. Following reconstruction of two-dimensional maximum projection images, spines were manually outlined, and length, width, area, density were measured in MetaMorph software (Molecular Devices, Sunnyvale, California) and subjected to statistical analysis (Student's *t* test). For each condition, a 100 μm dendritic region from each of 10-20 neurons each from 3 experiments were analyzed.

Nissl staining of mouse brains

Mice carrying the *Kalrn* null mutation were generated by replacing exons 27 and 28 of the *Kalrn* gene with a *neo* cassette, and have been described previously^{18, 21}. Twelve-week-old mice were anesthetized with a ketamine/xylazine mixture and perfused transcardially with PBS followed by 4% paraformaldehyde (PFA) in PBS. Brains were removed, postfixed overnight in 4% PFA/PBS, and cryoprotected in 30% sucrose/PBS. Brains were then cryosectioned at 50 μm and mounted on slides. Slides were passed through a graded series of ethanol solutions before being stained with a solution containing 0.625% cresyl violet acetate and 0.375% acetic acid. Slides were then dehydrated and mounted with Permount (Fisher Scientific, Pittsburgh, Pennsylvania).

Cortical neuropil analysis

Cortical neuropil in mice was quantified using semiautomatic image analysis. The temporal association area from 5-6 Nissl-stained sections 300 μm apart between bregma -1.82 mm and -3.40 mm, on either side of the midline, and were imaged with a 10× objective (NA 0.17, lateral resolution 0.633 μm/pixel). Analysis was performed remotely using ImageJ, with the experimenter blind to conditions. Images of layer 2/3, 4, and 5 were first thresholded to separate neurons from background. Because of possible variations in staining, images were thresholded automatically on a per-image basis. Images were then made into binary images, and glia were excluded by filtering objects smaller than 100 μm. The density of neuronal cell bodies in each image was quantified for each genotype, and neuropil size was defined as the percent of the area of each image not occupied by cell bodies. Both hemispheres from 5-6 sections were analyzed from three to four mice per genotype.

MR image collection and processing

T_1 -weighted MPAGE scans were collected on a Siemens 3T TIM TRIO imaging system (Siemens Medical Systems, Malvern, Pennsylvania) with $1\text{ mm} \times 1\text{ mm} \times 1\text{ mm}$ resolution. The MRI scans were processed with the Freesurfer (FS) image analysis suite release 4.1.0⁶⁹ (<http://surfer.nmr.mgh.harvard.edu>), which produced surface tessellations at the gray/white matter interface and the gray/CSF interface. FS provided 72 cortical regions of interest (ROI) based on a standard parcellation atlas⁷⁰, along with measures of cortical gray matter thickness (mm) for each of these regions using embedded FS algorithms.

Statistical analysis

Differences between the *KALRN*-variant-bearing individual with schizophrenia (*KALRN*-SCZ) and SCZ population were evaluated by generating standard (Z) scores for each cortical parcellation on the cortical thickness. Significance was defined as $p < 0.05$. Due to the exploratory nature of this analysis, scores were not corrected for multiple comparisons. Sign tests were performed to determine the relative placement of the *KALRN*-SCZ raw score (x_K) in relation to the SCZ and CON mean values. Sign was evaluated by applying the following:

$$\text{sign} \left(\frac{x_K - \mu_{SCZ}}{\mu_{SCZ} - \mu_{CON}} \right)$$

Where x_K is the *KALRN*-SCZ raw score, and μ_{SCZ} and μ_{CON} are the schizophrenic and

control population means, respectively. If $\frac{x_K - \mu_{SCZ}}{\mu_{SCZ} - \mu_{CON}} > 0$, then $\text{sign} = 1$, denoting the *KALRN*-SCZ value for that anatomical region and measure, x_K , is further away from μ_{CON}

than μ_{SCZ} is from μ_{CON} in either the positive or negative direction. If $\frac{x_K - \mu_{SCZ}}{\mu_{SCZ} - \mu_{CON}} < 0$, then $\text{sign} = -1$, which signified a value of x_K that is closer to μ_{CON} than μ_{SCZ} is to μ_{CON} . As we were interested in values of x_K that were accentuations of the SCZ phenotype, i.e. deviations from μ_{CON} in the extreme, we identified areas and measures of interest as those where $p(x_K) < 0.05$ and $\text{sign} = 1$.

This process was repeated to establish similar relationships between the *KALRN*-variant-bearing sibling (*KALRN*-SIB) and the SCZ-SIB population.

Supplementary Material

Refer to Web version on PubMed Central for supplementary material.

Acknowledgments

This work was supported by grants from the NIH-NIMH to P.P. (MH071316 and MH097216) and to L.W. and J.G.C. (MH071616, and MH084803).

References

1. Nimchinsky EA, Sabatini BL, Svoboda K. Structure and function of dendritic spines. *Annual review of physiology*. 2002; 64:313–353.
2. Lamprecht R. Actin cytoskeleton in memory formation. *Progress in neurobiology*. 2014
3. Penzes P, Rafalovich I. Regulation of the actin cytoskeleton in dendritic spines. *Advances in experimental medicine and biology*. 2012; 970:81–95. [PubMed: 22351052]
4. Feldman DE. Synaptic mechanisms for plasticity in neocortex. *Annu Rev Neurosci*. 2009; 32:33–55. [PubMed: 19400721]
5. Lamprecht R, LeDoux J. Structural plasticity and memory. *Nat Rev Neurosci*. 2004; 5:45–54. [PubMed: 14708003]
6. Fiala JC, Spacek J, Harris KM. Dendritic spine pathology: cause or consequence of neurological disorders? *Brain research Brain research reviews*. 2002; 39:29–54. [PubMed: 12086707]
7. Penzes P, Cahill ME, Jones KA, VanLeeuwen JE, Woolfrey KM. Dendritic spine pathology in neuropsychiatric disorders. *Nat Neurosci*. 2011; 14:285–293. [PubMed: 21346746]
8. Bennett MR. Schizophrenia: susceptibility genes, dendritic-spine pathology and gray matter loss. *Progress in neurobiology*. 2011; 95:275–300. [PubMed: 21907759]
9. Tolia K, Duman JG, Um K. Control of synapse development and plasticity by Rho GTPase regulatory proteins. *Progress in neurobiology*. 2011; 94:133–148. [PubMed: 21530608]
10. Carlisle HJ, Kennedy MB. Spine architecture and synaptic plasticity. *Trends Neurosci*. 2005; 28:182–187. [PubMed: 15808352]
11. Penzes P, Jones KA. Dendritic spine dynamics--a key role for kalirin-7. *Trends Neurosci*. 2008; 31:419–427. [PubMed: 18597863]
12. Johnson RC, Penzes P, Eipper BA, Mains RE. Isoforms of kalirin, a neuronal Dbl family member, generated through use of different 5'- and 3'-ends along with an internal translational initiation site. *J Biol Chem*. 2000; 275:19324–19333. [PubMed: 10777487]
13. Rabiner CA, Mains RE, Eipper BA. Kalirin: a dual Rho guanine nucleotide exchange factor that is so much more than the sum of its many parts. *Neuroscientist*. 2005; 11:148–160. [PubMed: 15746383]
14. Penzes P, Johnson RC, Alam MR, Kambampati V, Mains RE, Eipper BA. An isoform of kalirin, a brain-specific GDP/GTP exchange factor, is enriched in the postsynaptic density fraction. *J Biol Chem*. 2000; 275:6395–6403. [PubMed: 10692441]
15. Penzes P, et al. The neuronal Rho-GEF Kalirin-7 interacts with PDZ domain-containing proteins and regulates dendritic morphogenesis. *Neuron*. 2001; 29:229–242. [PubMed: 11182094]
16. Penzes P, et al. Rapid induction of dendritic spine morphogenesis by trans-synaptic ephrinB-EphB receptor activation of the Rho-GEF kalirin. *Neuron*. 2003; 37:263–274. [PubMed: 12546821]
17. Xie Z, et al. Kalirin-7 controls activity-dependent structural and functional plasticity of dendritic spines. *Neuron*. 2007; 56:640–656. [PubMed: 18031682]
18. Xie Z, Cahill ME, Penzes P. Kalirin loss results in cortical morphological alterations. *Mol Cell Neurosci*. 2010; 43:81–89. [PubMed: 19800004]
19. Hayashi-Takagi A, et al. Disrupted-in-Schizophrenia 1 (DISC1) regulates spines of the glutamate synapse via Rac1. *Nat Neurosci*. 2010; 13:327–332. [PubMed: 20139976]
20. Cahill ME, et al. Control of interneuron dendritic growth through NRG1/erbB4-mediated kalirin-7 disinhibition. *Mol Psychiatry*. 2011
21. Cahill ME, et al. Kalirin regulates cortical spine morphogenesis and disease-related behavioral phenotypes. *Proc Natl Acad Sci U S A*. 2009; 106:13058–13063. [PubMed: 19625617]
22. Kushima I, et al. Resequencing and Association Analysis of the KALRN and EPHB1 Genes And Their Contribution to Schizophrenia Susceptibility. *Schizophr Bull*. 2010
23. Hill JJ, Hashimoto T, Lewis DA. Molecular mechanisms contributing to dendritic spine alterations in the prefrontal cortex of subjects with schizophrenia. *Mol Psychiatry*. 2006; 11:557–566. [PubMed: 16402129]
24. Rubio MD, Haroutunian V, Meador-Woodruff JH. Abnormalities of the Duo/Ras-related C3 botulinum toxin substrate 1/p21-activated kinase 1 pathway drive myosin light chain

- phosphorylation in frontal cortex in schizophrenia. *Biol Psychiatry*. 2012; 71:906–914. [PubMed: 22458949]
25. Fromer M, et al. De novo mutations in schizophrenia implicate synaptic networks. *Nature*. 2014; 506:179–184. [PubMed: 24463507]
 26. Purcell SM, et al. A polygenic burden of rare disruptive mutations in schizophrenia. *Nature*. 2014; 506:185–190. [PubMed: 24463508]
 27. Adzhubei IA, et al. A method and server for predicting damaging missense mutations. *Nature methods*. 2010; 7:248–249. [PubMed: 20354512]
 28. Penzes P, Cahill ME. Deconstructing signal transduction pathways that regulate the actin cytoskeleton in dendritic spines. *Cytoskeleton (Hoboken)*. 2012; 69:426–441. [PubMed: 22307832]
 29. Eichler EE, et al. Completing the map of human genetic variation. *Nature*. 2007; 447:161–165. [PubMed: 17495918]
 30. Iafrate AJ, et al. Detection of large-scale variation in the human genome. *Nat Genet*. 2004; 36:949–951. [PubMed: 15286789]
 31. Duan J, Sanders AR, Gejman PV. Genome-wide approaches to schizophrenia. *Brain research bulletin*. 2010; 83:93–102. [PubMed: 20433910]
 32. Myers RA, et al. A population genetic approach to mapping neurological disorder genes using deep resequencing. *PLoS Genet*. 2011; 7:e1001318. [PubMed: 21383861]
 33. Sebat J, Levy DL, McCarthy SE. Rare structural variants in schizophrenia: one disorder, multiple mutations; one mutation, multiple disorders. *Trends Genet*. 2009; 25:528–535. [PubMed: 19883952]
 34. Glessner JT, et al. Strong synaptic transmission impact by copy number variations in schizophrenia. *Proc Natl Acad Sci U S A*. 2010; 107:10584–10589. [PubMed: 20489179]
 35. Li N, et al. mTOR-dependent synapse formation underlies the rapid antidepressant effects of NMDA antagonists. *Science*. 2010; 329:959–964. [PubMed: 20724638]
 36. Lee SH, et al. Genetic relationship between five psychiatric disorders estimated from genome-wide SNPs. *Nat Genet*. 2013; 45:984–994. [PubMed: 23933821]
 37. Identification of risk loci with shared effects on five major psychiatric disorders: a genome-wide analysis. *Lancet*. 2013; 381:1371–1379. [PubMed: 23453885]
 38. Andreassen OA, et al. Genetic pleiotropy between multiple sclerosis and schizophrenia but not bipolar disorder: differential involvement of immune-related gene loci. *Mol Psychiatry*. 2014
 39. Andreassen OA, et al. Improved detection of common variants associated with schizophrenia by leveraging pleiotropy with cardiovascular-disease risk factors. *Am J Hum Genet*. 2013; 92:197–209. [PubMed: 23375658]
 40. Silveira JM, Seeman MV. Shared psychotic disorder: a critical review of the literature. *Canadian journal of psychiatry Revue canadienne de psychiatrie*. 1995; 40:389–395. [PubMed: 8548718]
 41. Herz MI, Melville C. Relapse in schizophrenia. *Am J Psychiatry*. 1980; 137:801–805. [PubMed: 6104444]
 42. Meda SA, et al. Multivariate analysis reveals genetic associations of the resting default mode network in psychotic bipolar disorder and schizophrenia. *Proc Natl Acad Sci U S A*. 2014; 111:E2066–2075. [PubMed: 24778245]
 43. Cahill ME, Remmers C, Jones KA, Xie Z, Sweet RA, Penzes P. Neuregulin1 signaling promotes dendritic spine growth through kalirin. *Journal of neurochemistry*. 2013; 126:625–635. [PubMed: 23742124]
 44. Jones KA, Srivastava DP, Allen JA, Strachan RT, Roth BL, Penzes P. Rapid modulation of spine morphology by the 5-HT_{2A} serotonin receptor through kalirin-7 signaling. *Proc Natl Acad Sci U S A*. 2009; 106:19575–19580. [PubMed: 19889983]
 45. Cannon TD, et al. Association of DISC1/TRAX haplotypes with schizophrenia, reduced prefrontal gray matter, and impaired short- and long-term memory. *Arch Gen Psychiatry*. 2005; 62:1205–1213. [PubMed: 16275808]
 46. Carless MA, et al. Impact of DISC1 variation on neuroanatomical and neurocognitive phenotypes. *Mol Psychiatry*. 2011; 16:1096–1104. 1063. [PubMed: 21483430]

47. Lee FH, et al. Disc1 point mutations in mice affect development of the cerebral cortex. *J Neurosci*. 2011; 31:3197–3206. [PubMed: 21368031]
48. Lepagnol-Bestel AM, Kvjajo M, Karayiorgou M, Simonneau M, Gogos JA. A Disc1 mutation differentially affects neurites and spines in hippocampal and cortical neurons. *Mol Cell Neurosci*. 2013; 54:84–92. [PubMed: 23396153]
49. Tosato S, et al. Is neuregulin 1 involved in determining cerebral volumes in schizophrenia? Preliminary results showing a decrease in superior temporal gyrus volume. *Neuropsychobiology*. 2012; 65:119–125. [PubMed: 22378022]
50. Barros CS, et al. Impaired maturation of dendritic spines without disorganization of cortical cell layers in mice lacking NRG1/ErbB signaling in the central nervous system. *Proc Natl Acad Sci U S A*. 2009; 106:4507–4512. [PubMed: 19240213]
51. Meltzer HY, Massey BW, Horiguchi M. Serotonin receptors as targets for drugs useful to treat psychosis and cognitive impairment in schizophrenia. *Current pharmaceutical biotechnology*. 2012; 13:1572–1586. [PubMed: 22283753]
52. Dean B. Interpreting the significance of decreased cortical serotonin 2A receptors in schizophrenia. *Progress in neuro-psychopharmacology & biological psychiatry*. 2009; 33:1583–1584. author reply 1585–1586. [PubMed: 19699251]
53. Brunet-Gouet E, Achim AM, Vistoli D, Passerieux C, Hardy-Bayle MC, Jackson PL. The study of social cognition with neuroimaging methods as a means to explore future directions of deficit evaluation in schizophrenia? *Psychiatry Res*. 2011; 190:23–31. [PubMed: 21185085]
54. Gur RE, et al. Flat affect in schizophrenia: relation to emotion processing and neurocognitive measures. *Schizophr Bull*. 2006; 32:279–287. [PubMed: 16452608]
55. Karlsgodt KH, et al. Developmental disruptions in neural connectivity in the pathophysiology of schizophrenia. *Dev Psychopathol*. 2008; 20:1297–1327. [PubMed: 18838043]
56. Rapoport JL, et al. Progressive cortical change during adolescence in childhood-onset schizophrenia. A longitudinal magnetic resonance imaging study. *Arch Gen Psychiatry*. 1999; 56:649–654. [PubMed: 10401513]
57. Huttenlocher PR. Synaptic density in human frontal cortex - developmental changes and effects of aging. *Brain Res*. 1979; 163:195–205. [PubMed: 427544]
58. Glantz LA, Lewis DA. Decreased dendritic spine density on prefrontal cortical pyramidal neurons in schizophrenia. *Arch Gen Psychiatry*. 2000; 57:65–73. [PubMed: 10632234]
59. Glausier JR, Lewis DA. Dendritic spine pathology in schizophrenia. *Neuroscience*. 2013; 251:90–107. [PubMed: 22546337]
60. Selemon LD, Goldman-Rakic PS. The reduced neuropil hypothesis: a circuit based model of schizophrenia. *Biol Psychiatry*. 1999; 45:17–25. [PubMed: 9894571]
61. Lewis DA, Sweet RA. Schizophrenia from a neural circuitry perspective: advancing toward rational pharmacological therapies. *The Journal of clinical investigation*. 2009; 119:706–716. [PubMed: 19339762]
62. Ripke S, et al. Genome-wide association analysis identifies 13 new risk loci for schizophrenia. *Nat Genet*. 2013; 45:1150–1159. [PubMed: 23974872]
63. Sullivan PF, et al. Genomewide association for schizophrenia in the CATIE study: results of stage 1. *Mol Psychiatry*. 2008; 13:570–584. [PubMed: 18347602]
64. Ikeda M, et al. Genome-wide association study of schizophrenia in a Japanese population. *Biol Psychiatry*. 2011; 69:472–478. [PubMed: 20832056]
65. Calabrese DR, et al. Cingulate gyrus neuroanatomy in schizophrenia subjects and their non-psychotic siblings. *Schizophr Res*. 2008; 104:61–70. [PubMed: 18692994]
66. Delawalla Z, et al. Factors mediating cognitive deficits and psychopathology among siblings of individuals with schizophrenia. *Schizophr Bull*. 2006; 32:525–537. [PubMed: 16714471]
67. Srivastava DP, et al. Rapid enhancement of two-step wiring plasticity by estrogen and NMDA receptor activity. *Proc Natl Acad Sci U S A*. 2008; 105:14650–14655. [PubMed: 18801922]
68. Schneider CA, Rasband WS, Eliceiri KW. NIH Image to ImageJ: 25 years of image analysis. *Nature methods*. 2012; 9:671–675. [PubMed: 22930834]

69. Dale AM, Fischl B, Sereno MI. Cortical surface-based analysis. I. Segmentation and surface reconstruction. *Neuroimage*. 1999; 9:179–194. [PubMed: 9931268]
70. Desikan RS, et al. An automated labeling system for subdividing the human cerebral cortex on MRI scans into gyral based regions of interest. *Neuroimage*. 2006; 31:968–980. [PubMed: 16530430]

Author Manuscript

Author Manuscript

Author Manuscript

Author Manuscript

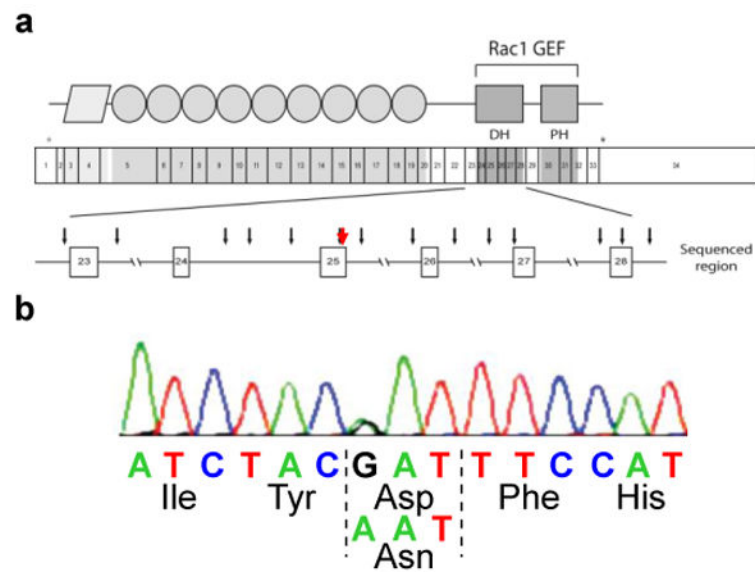


Figure 1.

Identification of the *KALRN* variant coding for kalirin-7 p.D1338N. **(a)** Schematic of the kalirin-7 protein (top), mRNA (middle), and the genomic regions that were sequenced. The catalytic Rac1-GEF domain, composed of Dbl-homology (DH) and pleckstrin-homology (PH) domains, is indicated. Fifteen distinct silent and intronic variants identified among 127 patients are denoted by black arrows, and the SNP leading to the p.D1338N variant is denoted by a red arrow. **(b)** Chromatogram illustrating that KAL-SZ is heterozygous for the minor allele (NC_000003.12:g.124462620G>A) responsible for the kalirin-7 coding variant. The chromatogram from KAL-SIB showed a similar result.

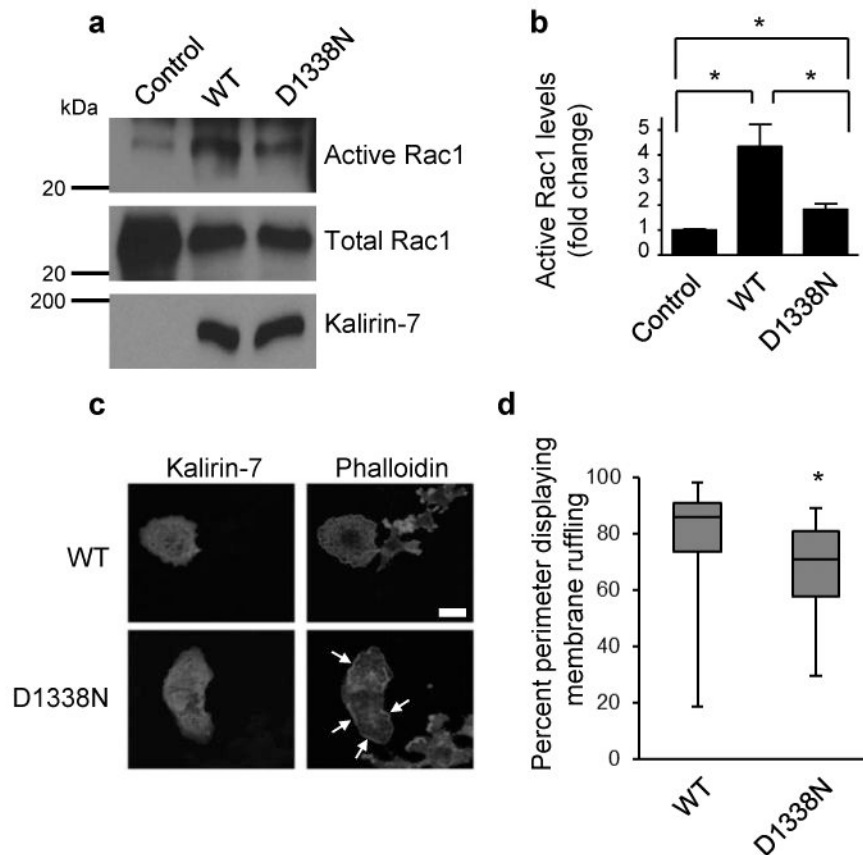


Figure 2.

Biochemical consequences of the D1338N variant. **(a, b)** Activation of Rac1 is attenuated in hEK-293 cells expressing kalirin-7-D1338N as compared to those expressing wildtype (WT) kalirin-7. Rac1-GTP was isolated by incubation of cell lysates with a GST-PAK binding domain fusion protein, and levels were normalized to total Rac1 and kalirin-7 expression. Three independent experiments were performed, each of which involved transfection of two wells of cells per condition. **(c, d)** COS-7 cells expressing myc-kalirin-7-D1338N (lower panels) exhibit a lesser degree of membrane ruffling, as visualized by staining with Alexa488-conjugated phalloidin, than do those expressing wildtype kalirin-7 (upper panels). The cell in the upper left panel displays ruffles on nearly 100% of its perimeter, whereas the cell in the lower left panel only displays ruffles in distinct locations (arrows). Analysis of 30-35 cells was performed for each condition. *: $P < 0.05$. Data are mean \pm SEM. Scale bar: 10 μ m.

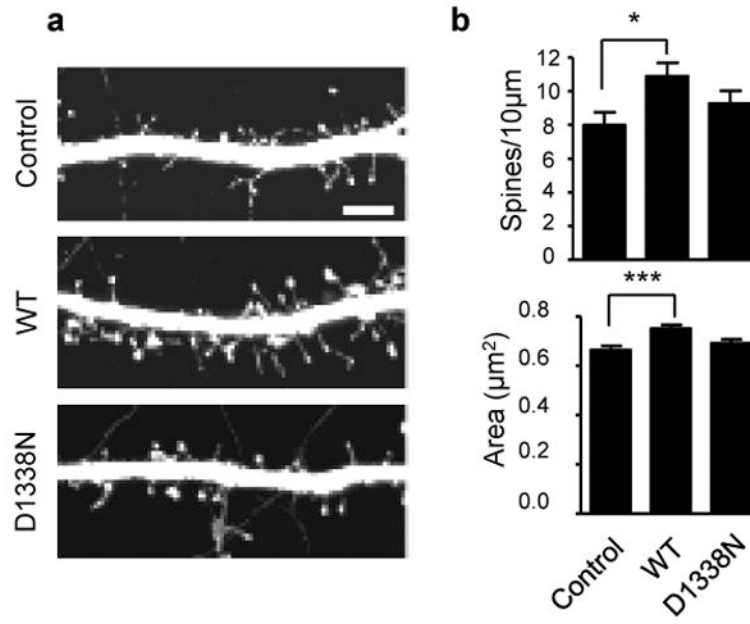


Figure 3.

Dendritic spine density and area following kalirin-7 transfection. (a) Rat cortical pyramidal neurons were transfected with an eGFP expression vector alone (top panel), or with wildtype kalirin-7 (middle panel) or kalirin-7-D1338N (bottom panel). (b) Quantification of spine density (upper panel) and spine area (lower panel) reveals an increase in both parameters in the neurons overexpressing wildtype kalirin-7. No change was seen following overexpression of kalirin-7-D1338N. *: $P < 0.05$; ***: $P < 0.001$. Data are mean \pm SEM. Scale bar: 5 μm .

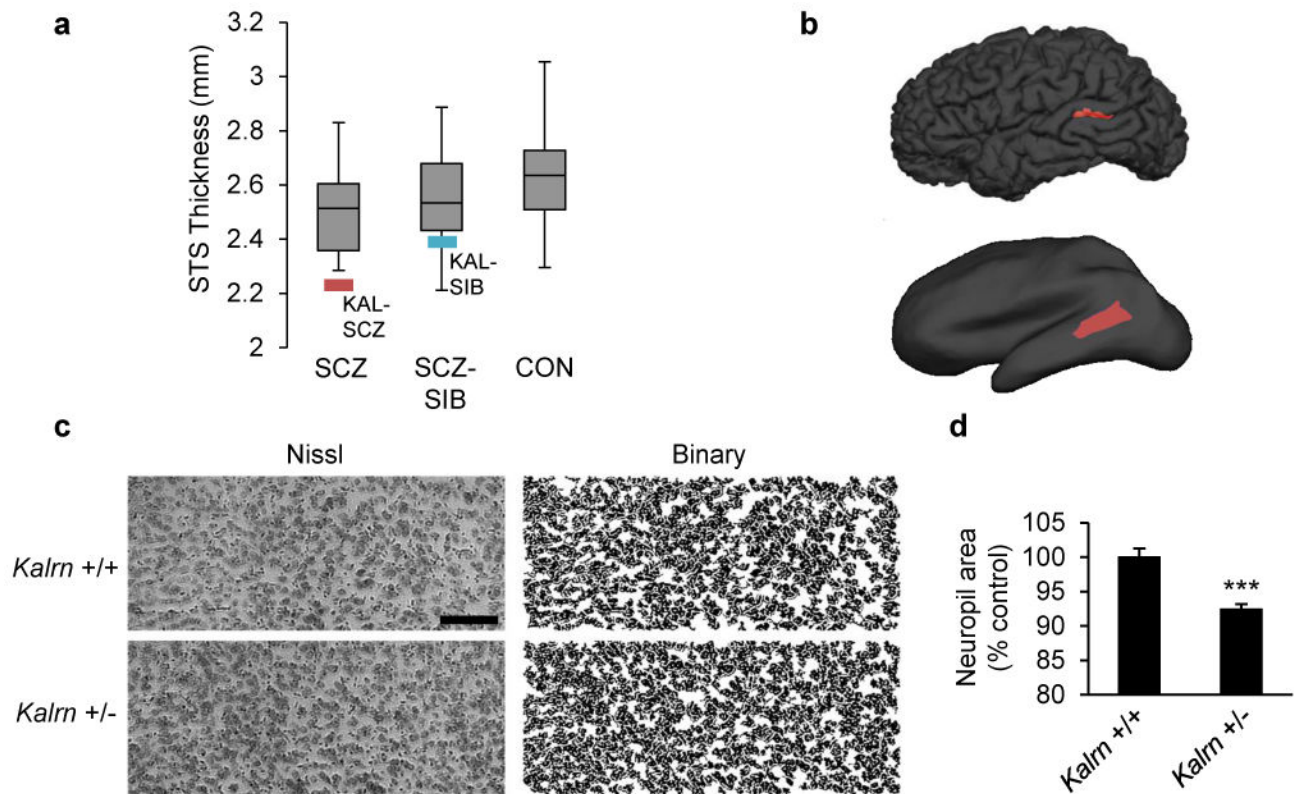


Figure 4.

Impact of kalirin-7 hypofunction on cortical thickness. **(a, b)** Both KAL-SCZ (red bar) and KAL-SIB (blue bar) had reduced cortical thickness in the left superior temporal sulcus (STS; location on pial and inflated surfaces illustrated in the upper and lower panels, respectively, of **(b)**) as compared to the means of their respective experimental groups. The STS thickness measurement for KAL-SCZ was 1.72 standard deviations lower than the SCZ group mean. **(c, d)** Quantification of neuropil area in the temporal association cortex of 12-week-old wildtype mice (**(c)**, upper panels) and litter-matched heterozygous *Kalrn*-null mice (**(c)** lower panels) revealed a reduction in neuropil in mice carrying only one functional *Kalrn* allele. Neuropil was calculated by performing Nissl staining (**(c)**, left panels), binarizing and filtering images of the tissue (**(c)**, right panels), and calculating the area of the images not occupied by neuronal somata. Eight to twelve images were acquired from each of three or four animals per genotype. ***: $P < 0.001$. Data are mean \pm SEM. Scale bar: 100 μ m.